Supporting Information

Takayama et al. 10.1073/pnas.1101459108

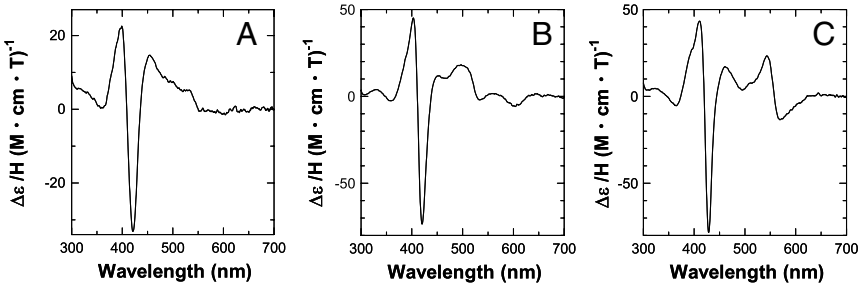

Fig. S1. Magnetic circular dichroism (MCD) spectra of IsdIFe^{3+} (10 μM, 20 °C). (*A*) low-pH form (pH 5.8) (*B*) high-pH form (pH 8.0), and (*C*) CN^- bound form (pH 8.0). Spectra were recorded with a Jasco Model J-720 spectropolarimeter equipped with an electromagnet (Alpha Magnetics) that generated a magnetic field of 1 T. MCD spectra were calculated from the difference between spectra obtained with parallel and antiparallel field orientations. The MCD spectra of low-pH, high-pH, and CN^- bound forms of IsdI are displayed in Fig. S1, and MCD parameters of the Soret band are compared with those of rat HO-1 in Table S1. The slight red-shift and increase in intensity of the Soret band was observed for all three forms of IsdI relative to HO-1, however, overall spectra pattern is similar in each, indicating that the axial ligand of IsdI is identical to HO-1, which is water at low-pH and hydroxide at high-pH.

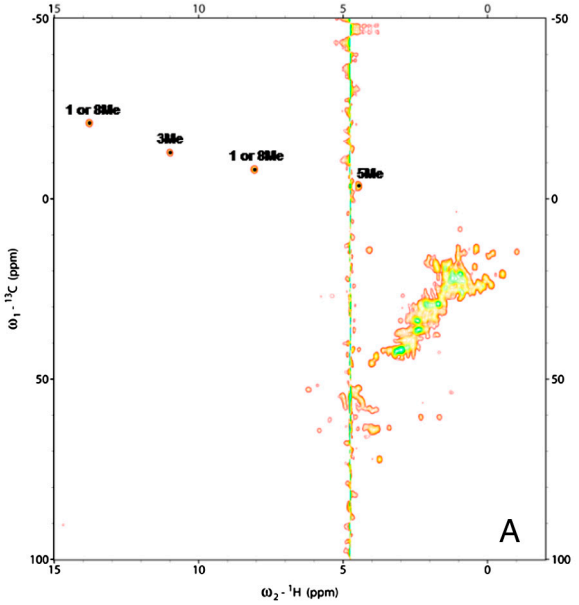
1 or 8Me
3Me
1 or 8Me
5Me
A
ω_1 - ^{13}C (ppm)
ω_2 - ^{1}H (ppm)

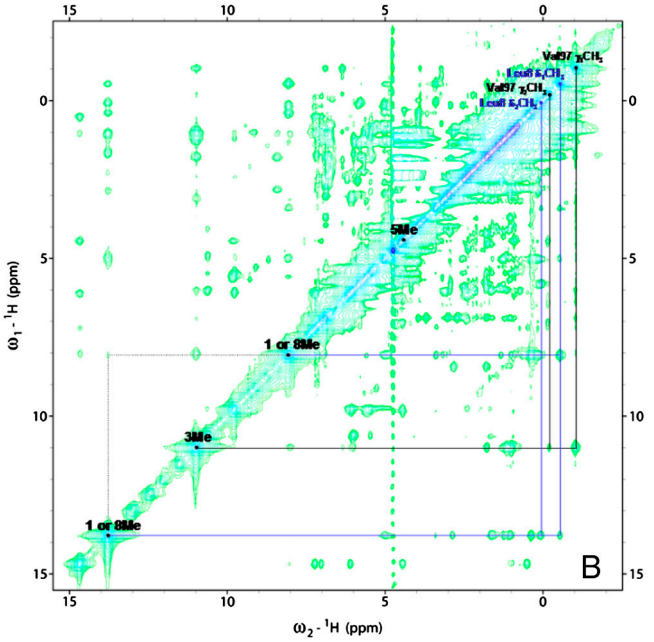
Val97 γ1CH3
Val97 γ2CH3
Leu8 δ2CH3
Leu8 δ1CH3
5Me
1 or 8Me
3Me
1 or 8Me
B
ω_1 - ^{1}H (ppm)
ω_2 - ^{1}H (ppm)

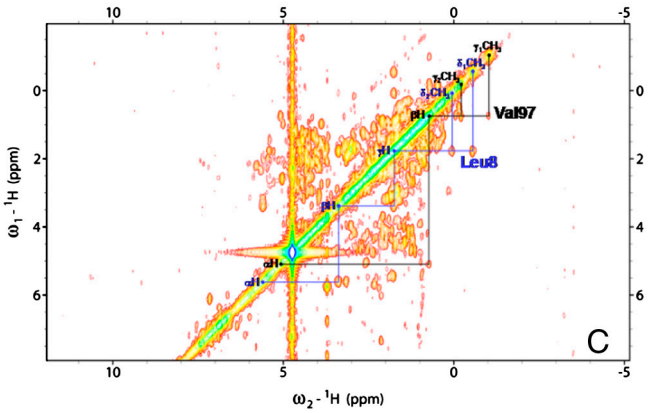
γ1CH3
δ2CH3
γ2CH3
δ1CH3
βH
Val97
αH
Leu8
C
ω_1 - ^{1}H (ppm)
ω_2 - ^{1}H (ppm)

Fig. S2. Two-dimensional ^{1}H NMR spectra. NMR experiments were performed with a Varian INOVA 500 MHz spectrometer. Phase sensitive NOESY spectra were recorded with mixing times of 15–40 ms. The ^{1}H-^{13}C heteronuclear multiple quantum coherence (HMQC) spectra were recorded with a refocusing time of 2.5 ms. COSY experiments were performed in the magnitude mode. All 2D spectra were collected with 2048 data points in the t_2 dimension and 256 or 512 blocks in the t_1 dimension with 512 scans/block (25 or 30 °C).

The ^{1}H NMR signal assignment of the High-pH form of IsdIFe^{3+} NOESY, COSY, and ^{1}H-^{13}C HMQC spectra (30 °C) are shown (Fig. S2) for the enzyme (1–2 mM) in sodium phosphate buffer (20 mM, 100% D_2O, pD 8.2, 30 °C). In the HMQC spectrum, four strong signals observed in the high-field region of the ^{13}C axis (<0 ppm, Fig. S2*A*) were assigned to the four heme methyl groups. Observation of a cross-peak between the signals at 13.8 and 8.1 ppm in the NOESY spectrum indicated that these signals are attributable to either the 1- or 8-methyl groups (Fig. S2*B*; mixing time, 15 ms). The finding that these two heme methyl signals both exhibit a cross-peak to the strong 3 proton signal at −0.5 ppm support this assignment by demonstrating the proximity of these two groups. The spin system assignment from the COSY spectrum indicated that the strong signal at −0.5 ppm is attributable to a $\delta - CH_3$ leucine and another $\delta - CH_3$ signal is at 0.1 ppm (Fig. S2*C*). The X-ray crystal structure of IsdI (6) indicated that Leu8 is located in close proximity to the heme 1-and 8-methyl residues, so the chemical shifts at 0.1 and −0.5 ppm were assigned to the δCH_3 group of Leu8. The observation of a cross-peak between the γCH_3 signal at 0.1 ppm and the heme methyl resonance at 13.8 ppm in the NOESY spectrum further support this assignment (Fig. S2*B*). The COSY experiment also suggests that the two other strong signals observed in the high-field region at −0.2 and −1.0 ppm are γCH_3 signals from the same valine residue (Fig. S2*C*). The X-ray crystal structure (1) indicates the presence of two valine residues near the heme, Val79, which is located in close proximity of the heme 1- and 8-methyl groups, and Val97, which is near the 3-methyl group. Both the −0.2 and −1.0 ppm signals exhibit a cross-peak to the heme methyl resonance at 11.0 ppm but not to either the 1- or 8-methyl groups in NOESY spectrum; therefore, the chemical shifts at −0.2 and −1.0 are assigned to be γCH_3 signals of Val97 and the resonance at 11.0 ppm is assigned to the heme 3-methyl group (Fig. S2*B*). The remaining heme methyl signal at 4.5 ppm is assigned to the 5-methyl group. The spin connectivities of Leu8 (blue) and Val97 (black) are indicated.

1 Reniere ML, et al. (2010) The IsdG-family of haem oxygenases degrades haem to a novel chromophore. *Mol Microbiol* 75:1529–1538.

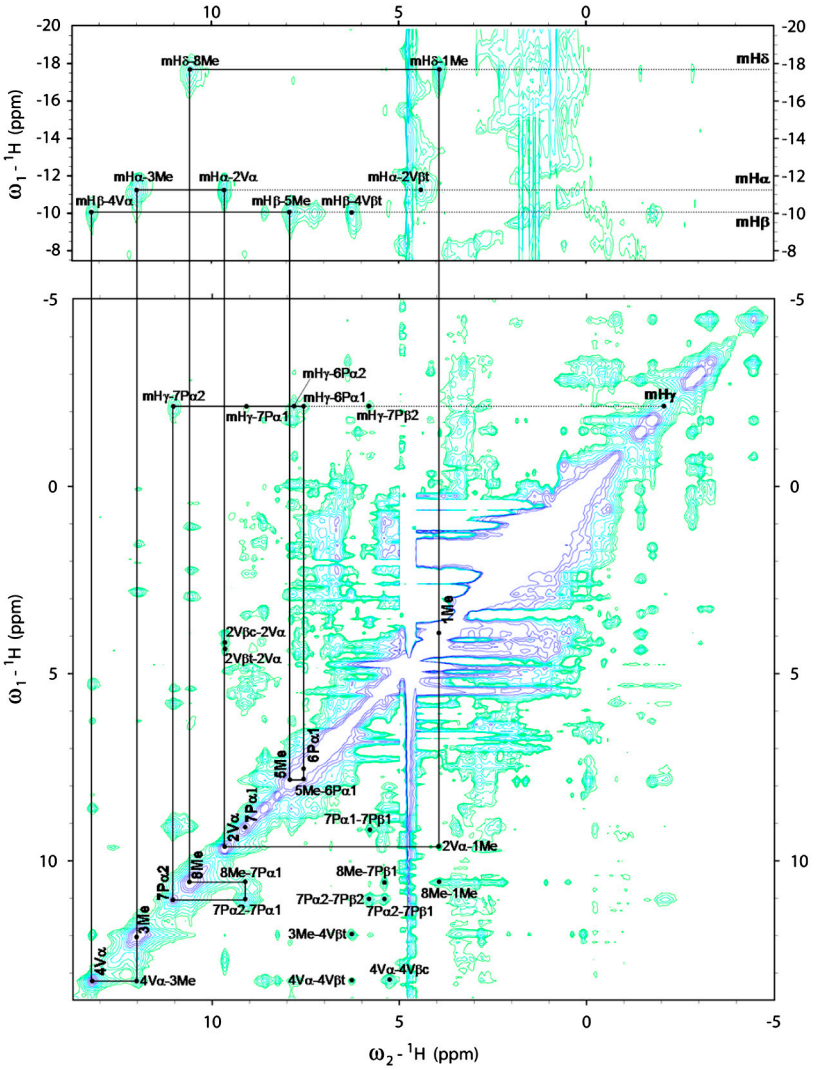

Fig. S3. The ^{1}H NMR assignments of IsdIFe^{3+}CN$^-$. IsdIFe^{3+}CN was prepared by adding a small crystal of potassium cyanide (KCN) to the IsdIFe^{3+}(high-pH) NMR sample. The NOESY spectrum of IsdIFe^{3+}CN (25 °C, mixing time, 15 ms) is shown. The broad single proton resonance at −17.6 ppm displays strong connectivity with the heme methyl signal at 10.6 ppm and another intense resonance at 3.9 ppm. A weak cross-peak between the signals at 10.6 and 3.9 ppm was also observed, suggesting that the single proton at −17.6 ppm is *meso*-δ and that the strong signals at 10.6 and 3.9 ppm arise from 8-methyl or 1-methyl. The signal at 10.6 ppm also correlates to the signals at 11.0, 9.1, and 5.4 ppm. The signal at 11.0 ppm correlates strongly with the signal at 9.1 ppm and has COSY correlation between the signals at 5.8 and 5.4 ppm. Therefore, the heme methyl signal at 10.6 ppm was assigned to the 8-methyl and signals at 11.0, 9.1, 5.8, and 5.4 to 7-propionate Hα2, Hα1, Hβ2, and Hβ1, respectively. Assignment of the 8-methyl signal leads to the assignment of the signal at 3.9 ppm as 1-methyl. The 1-methyl signal correlates to the signal at 9.7 ppm, which in turn has COSY correlation between the signals at 4.4 and 4.2 ppm, so the signals at 9.7, 4.4, and 4.2 are assigned to 2-vinyl Hα, Hβt and Hβc, respectively. The 2-vinyl Hα and Hβt signal correlate to the broad single proton signal at −11.2 ppm, which was assigned to *meso*-α. The *meso*-α signal correlates strongly with the heme methyl signal at 12.0 ppm, indicating that this signal is 3-methyl. The 3-methyl signal correlates to the signals at 13.2 and 6.3 ppm. The signal at 13.2 ppm has COSY correlation between signals at 6.3 and 5.3 ppm, so these signals are assigned to 4-vinyl Hα, Hβt, and Hβc, respectively. The 4-vinyl Hα and Hβt signals also correlate with a broad single proton signal at −10.0 ppm that is assigned to *meso*-β. The *meso*-β signal exhibits a strong cross-peak with the intense signal at 7.9 ppm, indicating that this signal arises from the 5-methyl group. The 5-methyl signal correlates with the signal at 7.5 ppm, and this signal and 7-propionate Hα1, Hα2, and Hβ2 signals all correlate to the broad signal at −2.1 ppm. Thus, the signals at 7.5 and −2.1 ppm were assigned to 6-propionate Hα1 and *meso*-γ, respectively. These assignments are summarized in Table S3.

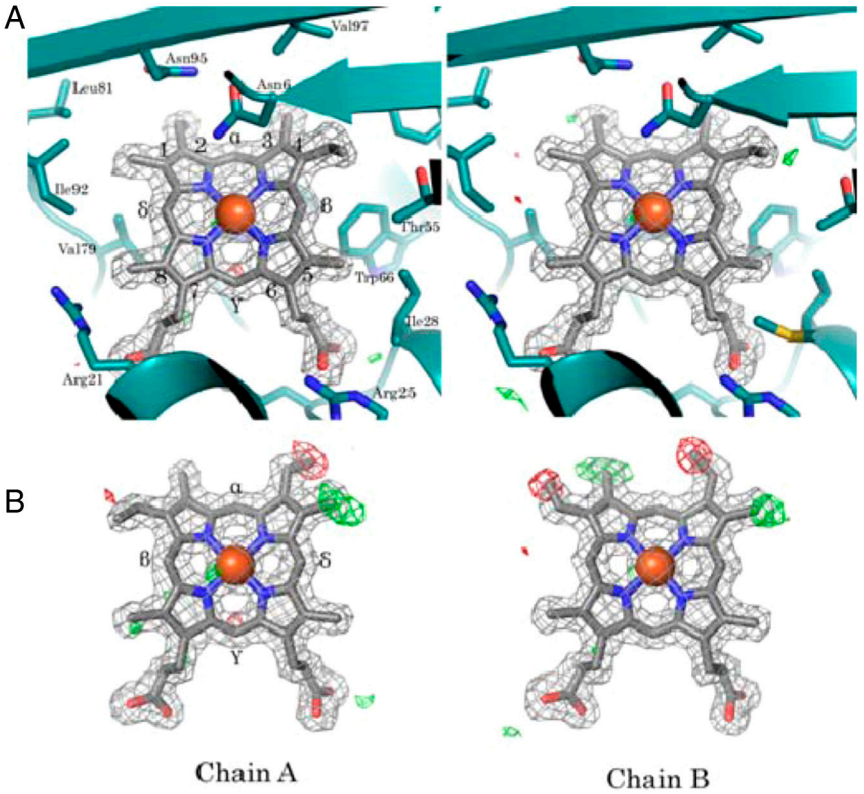

Fig. S4. The difference density for the two possible heme orientations in IsdIFe^{3+}CN for both chains *A* and *B*. The $2F_o$-F_c map is represented as a mesh (gray) contoured at 1 σ. The F_o-F_c difference maps are contoured at 3 σ for positive (green) and negative (red) peaks. Heme *meso*-carbons are labeled. A. The heme orientation in the structure (Fig. 3). B. The heme modeled as flipped along the α/γ-meso carbon axis.

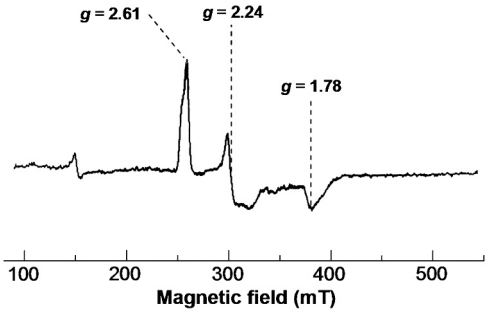

Fig. S5. X-band EPR spectrum (10 K) of IsdIFe^{3+} (pH 8.0; 170 μM). The spectrum was recorded with a Bruker ESP 300E spectrometer fitted with an Oxford Instruments Model 900 liquid helium cryostat, an Oxford Instruments ITC4 temperature controller, and a Hewlett-Packard model 5352B frequency counter. The *g*-values ($g = 2.61, 2.24, 1.78$) obtained from this spectrum are similar to those of rat HO-1 [$g = 2.67, 2.21, 1.79(1)$] measured at pH 9.0 and 4 K, indicating that the electronic state of high-pH form of IsdIFe^{3+} is similar to that of HO-1 at cryogenic temperature.

1 Takahashi S, *et al.* (1994) Heme-heme oxygenase complex. Structure of the catalytic site and its implication for oxygen activation. *J. Biol. Chem.* 269:1010–1014

Table S1. Electronic absorption and MCD parameters for IsdI and HOs

Absorption spectra

Protein	λ max (nm)		pK_a	λ max (nm)
	(Low pH)	(High pH)		(CN^- bound)
IsdI	404, 640	412, 485, 520, 578	7.1	421, 558
Rat HO-1	404, 500, 631 (1)	413, 540, 575 (1)	7.6 (1)	418, 536 (2)
Human HO-2	404, 500, 631 (3)	413, 540, 575 (3)	8.5 (3)	—
pa-HO	405, 503, 537, 638 (4)	415, 540, 574 (5)	8.1 (5)	419, ~540 (4)
nm-HO	405, 504, 638 (4)		9.3 (4)	419, ~540 (4)

MCD spectra

Protein	Λ* (Δε) †		
	peak	cross-over	trough
Low-pH form			
IsdI ‡	399 (+23)	409 (0)	421 (−33)
Rat HO-1 §	399 (+20)	407 (0)	416 (−11)
High-pH form			
IsdI ‡	403 (+45)	411 (0)	420 (−73)
Rat HO-1 §	402 (+35)	412 (0)	419 (−41)
CN^- bound form			
IsdI	411 (+43)	420 (0)	429 (−78)
Rat HO-1 §	406 (+52)	415 (0)	423 (−65)

*M^{-1} cm^{-1} T^{-1}.

†M^{-1} cm^{-1} T^{-1}.

‡This work, measured at 20 °C.

§Ref. 6, measured at 4 °C.

1 Takahashi S, et al. (1994) Heme–heme oxygenase complex. Structure of the catalytic site and its implication for oxygen activation. *J Biol Chem* 269:1010–1014.

2 Hawkins BK, Wilks A, Powers LS, Ortiz de Montellano PR, Dawson JH (1996) Ligation of the iron in the heme–heme oxygenase complex: X-ray absorption, electronic absorption, and magnetic circular dichroism studies. *Biochim Biophys Acta* 1295:165–173.

3 Ishikawa K, et al. (1995) Heme oxygenase-2. *J Biol Chem* 270:6345–6350.

4 Zeng Y, et al. (2005) Azide-inhibited bacterial heme oxygenases exhibit an $S = 3/2(d_{xz},d_{yz})^3(d_{xy})^1(d_{z2})^1$ spin state: Mechanistic implications for heme oxidation. *J Am Chem Soc* 127:9794–9807.

5 Caignan GA, et al. (2003) The hydroxide complex of *Pseudomonas aeruginosa* heme oxygenase as a model of the low-spin iron(III) hydroperoxide intermediate in heme catabolism: ^{13}C NMR spectroscopic studies suggest the active participation of the heme in macrocycle hydroxylation. *J Am Chem Soc* 125:11842–11852.

6 Hawkins BK, Wilks A, Powers LS, Ortiz de Montellano PR, Dawson JH (1996) Ligation of the iron in the heme-heme oxygenase complex: X-ray absorption, electronic absorption and magnetic circular dichroism studies. *Biochim Biophys Acta* 1295:165–173, measured at 4 °C.

Table S2. Heme protein methyl and *meso*-H chemical shifts

Protein	Temp. (°C)	Methyl shifts (ppm)	Av. (ppm)	Meso-H shifts (ppm)	Av. (ppm)	Reference
Hydroxide bound form						
IsdI	30	13.8, 10.9, 8.1, 4.5	9.3			This work
pa-HO	25	24, 17, 14, (10) *	(12.3) *			1
nm-HO	25	19.5, 17.5, 8.0, (7.0) *	(16.3) *			2
Nitrophorin2	30	19.0, 13.0, 10.7, 6.5	12.3			3
SW Mb	25	38.1, 38.1, 33.6, 26.8	34.1			4
Cyanide bound form						
IsdI	30	12.0, 10.6, 8.0, 4.0	8.7	−1.7, −9.5, −10.7, −16.8	−9.7	This work
human HO-1 †	25	19.6, 10.5, 9.0, 5.0	11.0	7.6, 7.1, 3.8, −5.1	3.4	5
pa-HO	10	27.7, 22.7, 19.0, 4.4	18.5	9.0, 8.6, −2.2, −2.5	3.2	6
nm-HO	25	21.4, 10.3, 9.6, 7.9	12.3			2
cd-HO	35	19.2, 10.6, 8.5, 5.4	10.9	8.2, 7.8, 2.4, −2.6	4.0	6
HmuO	25	19.7, 10.4, 8.1, 4.9	10.8	7.2, −3.6		7
Nitrophorin2	35	18.1, 13.4, 9.1, 7.6	12.1	5.6, 2.3, 2.3, −1.6	2.2	8
SW Mb	25	27.0, 18.6, 12.9, 4.8	15.8	6.0, 4.4, 4.1, 2.1	4.2	9

*Ref. 3.

†Protein reconstituted with protohemin.

1 Caignan GA, et al. (2003) The hydroxide complex of *Pseudomonas aeruginosa* heme oxygenase as a model of the low-spin iron(III) hydroperoxide intermediate in heme catabolism: ^{13}C NMR spectroscopic studies suggest the active participation of the heme in macrocycle hydroxylation. *J Am Chem Soc* 125:11842–11852.

2 Ma L-H, Liu Y, Zhang X, Yoshida T, La Mar GN (2006) ^{1}H NMR study of the magnetic properties and electronic structure of the hydroxide complex of substrate-bound heme oxygenase from *Neisseria meningitidis*: Influence of the axial water deprotonation on the distal H-bond network. *J Am Chem Soc* 128:6657–6668.

3 Shokhireva TK, Berry RE, Zhang H, Shokhirev NV, Walker FA (2008) Assignment of ferriheme resonances for high- and low-spin forms of nitrophorin 3 by ^{1}H and ^{13}C NMR spectroscopy and comparison to nitrophorin 2: Heme pocket structural similarities and differences. *Inorg Chim Acta* 361:925–940.

4 Koshikawa K, Yamamoto Y, Kamimura S, Matsuoka A, Shikama K (1998) NMR study of dynamics and thermodynamics of acid-alkaline transition in ferric hemoglobin of a midge larva (*Tokunagayusurika akamusi*). *Biochim Biophys Acta* 1385:89–100.

5 Gorst CM, Wilks A, Yeh DC, Ortiz de Montellano PR, La Mar GN (1998) Solution ^{1}H NMR investigation of the molecular and electronic structure of the active site of substrate-bound human heme oxygenase: The nature of the distal hydrogen bond donor to bound ligands. *J Am Chem Soc* 120:8875–8884.

6 Caignan GA, et al. (2002) Oxidation of heme to b- and d-biliverdin by *Pseudomonas aeruginosa* heme oxygenase as a consequence of an unusual seating of the heme. *J Am Chem Soc* 124:14879–14892.

7 Li Y, Syvitski RT, Chu GC, Ikeda-Saito M, Mar GNL (2003) Solution ^{1}H NMR investigation of the active site molecular and electronic structures of substrate-bound, cyanide-inhibited HmuO, a bacterial heme oxygenase from *Corynebacterium diphtheriae*. *J Biol Chem* 278:6651–6663.

8 Yang F, et al. (2009) ^{1}H and ^{13}C NMR spectroscopic studies of the ferriheme resonances of three low-spin complexes of wild-type nitrophorin 2 and nitrophorin 2(V24E) as a function of pH. *J Biol Inorg Chem* 14:1077–1095.

9 Emerson SD, La Mar GN (1990) Solution structural characterization of cyanometmyoglobin: Resonance assignment of heme cavity residues by two-dimensional NMR. *Biochemistry* 29:1545–1556.

Table S3. The ^{1}H chemical shifts of the heme substituents of IsdIFe^{3+}-CN^{-} at 25 °C

Position	Shifts (ppm)	Position	Shifts (ppm)
1 methyl	3.9	*meso*-α	−11.2
3 methyl	12.0	*meso*-β	−10.0
5 methyl	7.9	*meso*-γ	−2.1
8 methyl	10.6	*meso*-δ	−17.6
2 vinyl α	9.7	6 propionate α	7.8, 7.5
2 vinyl β	4.4, 4.2	6 propionate β	3.3, 2.9
4 vinyl α	13.2	7 propionate α	11.0, 9.1
4 vinyl β	6.3, 5.3	7 propionate β	5.8, 5.4

Table S4. X-ray crystallography data collection and refinement statistics for IsdIFe^{3+}CN

Data collection*	
Resolution range (Å)	47.75–1.80
Space group	$P2_12_12_1$
Unit cell dimension (Å)	$a = 58.8$, $b = 65.9$, $c = 69.3$
Unique reflections	25604 (3686)
Completeness (%)	99.5 (99.7)
Average I/σI	16.8 (5.1)
Redundancy	6.7 (6.9)
R_{merge}	0.078 (0.370)
Refinement	
$R_{work}(R_{free})$	0.175 (0.196)
No. Atoms:	
Protein	1902
Solvent	254
Heme	86
Cyanide	4
Overall B-factor (Å^2)	17.1
Protein	15.9
Solvent	27.4
Heme	12.9
Cyanide	11.8
R.m.s.deviation	
Bond length (Å)	0.013
Bond angles (°)	1.255

*Values in parentheses are for the highest resolution shell.